

Dynamic Differential Hall Effect Sensor

TLE4925/TLE4925C

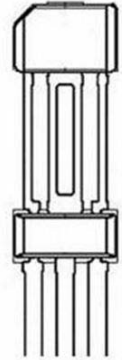
Data Sheet Version 6.0

Features

- High sensitivity
- Single chip solution
- Symmetrical thresholds
- High resistance to Piezo effects
- South and north pole pre-induction possible
- Low cut-off frequency
- Digital output signal
- Advanced performance by dynamic self calibration principle
- Two-wire and three-wire configuration possible
- Wide operating temperature range
- Fast start-up time
- Large operating air-gaps
- Reverse voltage protection at Vs- PIN
- Short- circuit and over temperature protection of output
- Digital output signal (voltage interface)
- Module style package with two 4.7nF integrated capacitors (TLE4925C)



PG-SSO-3-6



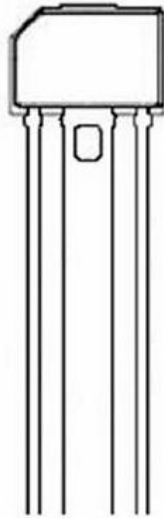
PG-SSO-3-9

| Type | Marking | Ordering Code | Package |
|----------|---------|---------------|------------|
| TLE4925 | 25 | Q62705-K677 | PG-SSO-3-6 |
| TLE4925C | 25C | Q62705-K676 | PG-SSO-3-9 |

General Information

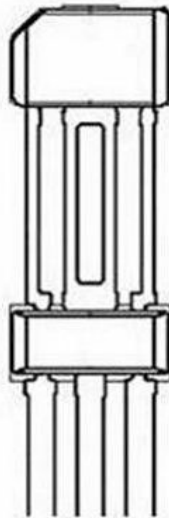
The TLE4925/TLE4925C is an active Hall sensor suited to detect the motion and position of ferromagnetic and permanent magnet structures. An additional self-calibration module has been implemented to achieve optimum accuracy during normal running operation. It comes in a three-pin package for the supply voltage and an open drain output.

PG-SSO-3-6



1 2 3

PG-SSO-3-9



1 2 3

Figure 1: Pin configuration in PG-SSO-3-6 and PG-SSO-3-9

Pin definition and Function

| Pin No. | Symbol | Function |
|---------|--------|-------------------|
| 1 | V_s | Supply Voltage |
| 2 | GND | Ground |
| 3 | Q | Open Drain Output |

Functional Description

The differential Hall sensor IC detects the motion and position of ferromagnetic and permanent magnet structures by measuring the differential flux density of the magnetic field. To detect ferromagnetic objects the magnetic field must be provided by a back biasing permanent magnet (south or north pole of the magnet attached to the rear unmarked side of the IC package).

Offset cancellation is achieved by advanced digital signal processing. Immediately after power-on motion is detected (start-up mode). After a few transitions the sensor has finished self-calibration and switches to a high-accuracy mode (running mode). In running mode switching occurs at signal zero-crossing of the arithmetic mean of max and min value of magnetic differential signal. ΔB is defined as difference between hall plate 1 and hall plate 2.

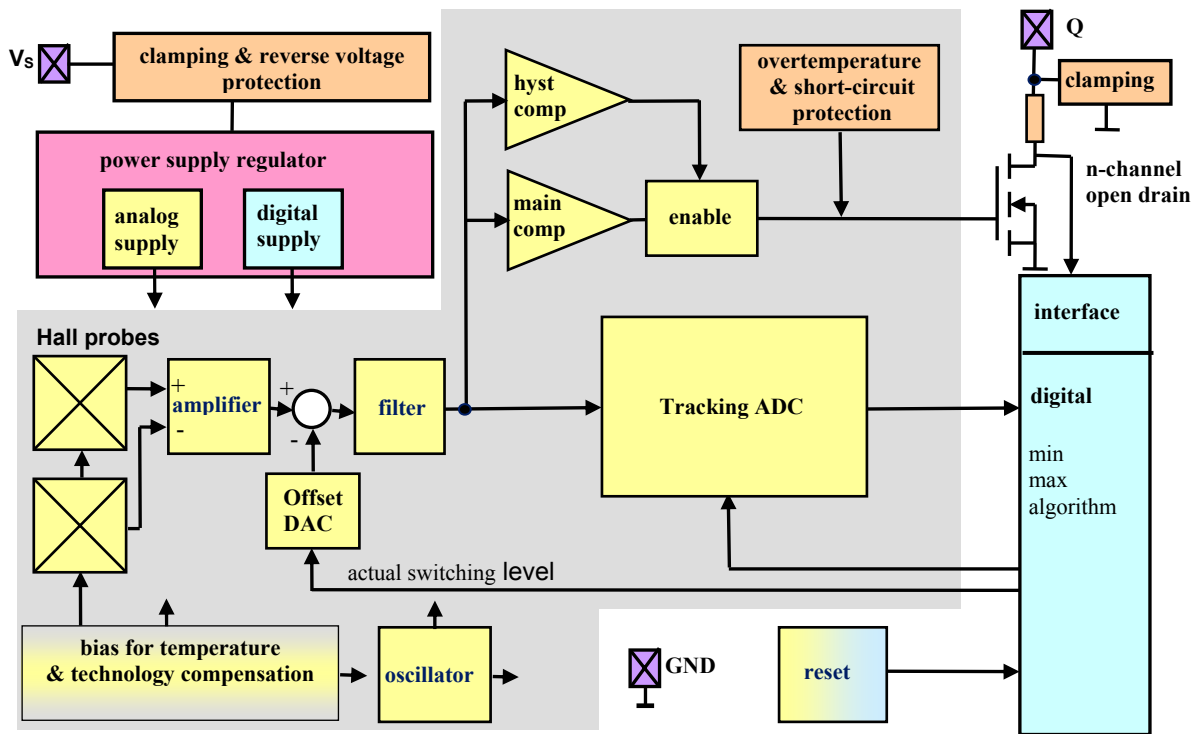


Figure 2: Block Diagram of TLE4925/TLE4925C

Circuit Description

The TLE4925/TLE4925C is comprised of a supply voltage regulator, a pair of hall probes, spaced at 2.5mm, differential amplifier, noise-shaping filter, comparator, advanced digital signal processor (DSP), A/D and D/A converter and an open drain output.

Startup mode:

The differential signal is digitized in the A/D converter and fed into the dsp part of the circuit. There a rising or falling transition is detected and the output stage is triggered accordingly. As the signal is not offset compensated at this time, the output does not necessarily switch at zero-crossing of the magnetic signal. Signal peaks are also detected in the digital circuit and their arithmetic mean value can be calculated. The offset of this mean value is determined and fed into the offset cancellation DAC. This procedure can be repeated with increasing accuracy. After few increments the IC is switched into the high accuracy running mode.

Running mode:

In running mode the output is triggered by the comparator. An offset cancellation feedback loop is formed by the A/D converter, dsp and offset cancellation D/A converter. In running mode switching always occurs at zero-crossing. It is only affected by the (small) remaining offset of the comparator and by the remaining propagation delay time of the signal path, mainly determined by the noise-shaping filter. Nevertheless signals below a defined threshold are not detected to avoid unwanted parasitic switching.

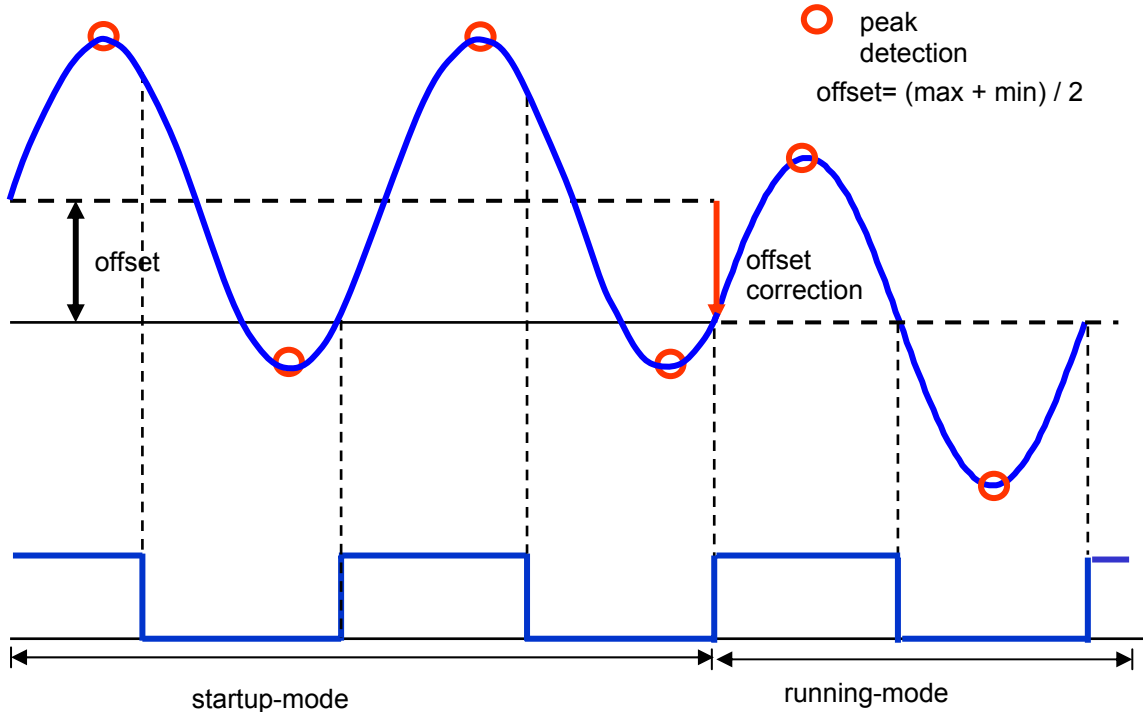


Figure 3: Startup of the device

At transition from startup-mode to running mode switching timing is moving from low-accuracy to high accuracy zero-crossing.

1.1 Absolute Maximum Ratings

| No. | Parameter | Symbol | min | Typ | max | Unit | Remarks |
|-------|--|-------------|------------------------------|-----|--------------------------|--|---|
| 1.1.1 | Supply voltage | V_S | -18 -24 -26 -28 | | 18 24 26 28 | V V V V | - 1h with $R_{Series} \geq 200\Omega^1$ 5min with $R_{Series} \geq 200\Omega^1$ 1min with $R_{Series} \geq 200\Omega^1$ |
| 1.1.2 | Supply current | I_S | -10 | | 25 | mA | - |
| 1.1.3 | Output OFF voltage | V_Q | -0.3 -0.3 -0.3 -1.0 | | 18 24 26 - | V V V V | - 1h with $R_{Load} \geq 500\Omega$ 5min with $R_{Load} \geq 500\Omega$ 1h (protected by internal series resistor) |
| 1.1.4 | Output ON voltage | V_Q | - - - | | 16 18 24 | V V V | Current internal limited by short circuit protection (72h @ $T_A < 40^\circ\text{C}$). Current internal limited by short circuit protection (1h @ $T_A < 40^\circ\text{C}$). Current internal limited by short circuit protection (1min @ $T_A < 40^\circ\text{C}$). |
| 1.1.5 | Continuous output current | I_Q | -50 | | 50 | mA | - |
| 1.1.6 | Junction temperature | T_j | -40 | | 155 165 175 195 | $^\circ\text{C}$ $^\circ\text{C}$ $^\circ\text{C}$ $^\circ\text{C}$ | - 2000h (not additive) 1000h (not additive) 168 h (not additive) 3 x 1 h (additive to the other life times). |
| 1.1.7 | Storage temperature | T_S | -40 | | 150 | $^\circ\text{C}$ | - |
| 1.1.8 | Thermal resistance junction-air for PG-SSO-3-6 PG-SSO-3-9 | $R_{th JA}$ | | | 190 | K/W | Lower values are possible with overmoulded devices. |

Note: Stresses above those listed here may cause permanent damage to the device. Exposure to absolute maximum rating conditions for extended periods may affect device reliability.

¹ Accumulated life time.

1.2 ESD Protection

| No. | Parameter | Symbol | | max | Unit | Remarks |
|-------|--|-----------|--|--------------------|----------|--|
| 1.2.1 | ESD – protection PG-SSO-3-9 PG-SSO-3-6 | V_{ESD} | | ± 6 ± 4 | kV kV | According to standard EIA/JESD22-A114-B Human Body Model (HBM 1500 Ohm/100pF) |

2.1 Operating Range

| No. | Parameter | Symbol | min | typ | max | Unit | Remarks |
|-------|-------------------------------|-----------|------|-----|-----|----------|---|
| 2.1.1 | Supply voltage | V_S | 3.3 | | 18 | V | Continuous |
| | | | | | 24 | V | 1h with $R_{Series} \geq 200\Omega$ |
| | | | | | 26 | V | 5min with $R_{Series} \geq 200\Omega$. Extended limits for parameters in characteristics. |
| | | | 3 | | | V | During test pulse 4. Limited performance possible |
| 2.1.2 | Supply voltage ripple | V_{SAC} | | | 6 | V_{pp} | $V_S=13V$; $0 < f < 50kHz$ |
| 2.1.3 | Continuous output OFF voltage | V_Q | -0.3 | | 18 | V | Continuous |
| | | | -18 | | 24 | V | 1h with $R_{Load} \geq 500\Omega$ |
| 2.1.4 | Continuous output ON current | I_Q | 0 | | 20 | mA | $V_{Qmax}=0.6V$ |
| 2.1.5 | Power on time | t_{on} | | | 1 | ms | Time to achieve specified accuracy After power on the output of the IC is always in high-state. After internal resets output is locked ² . |

² Output of the IC is locked in present state (high-state or low-state) after an internal reset is launched. This reset happens typically every 780ms when there is no significant signal change. See also 2.2.14. A voltage reset causes a release of the output and output is in high state after power on again.

| | | | | | | | |
|-------|--------------------------------|-------|-----|--|-----|----|---|
| 2.1.6 | Operating junction temperature | T_j | -40 | | | °C | - |
| | | | | | 155 | °C | 2000 h (not additive) |
| | | | | | 165 | °C | 1000 h (not additive) |
| | | | | | 175 | °C | 168 h (not additive) reduced signal quality permissible (e.g. jitter) |

*Note: Unless otherwise noted, all temperatures refer to junction temperature.
For the supply voltage lower than 28V ($R_{Series} \geq 200\Omega$) and junction temperature lower than 195°C the magnetic and AC/DC characteristics can exceed the specification limits.*

2.2 AC/DC Characteristics

Over operating range, unless otherwise specified. Typical values correspond to $V_S=12V$ and $T_A=25^\circ C$

| No. | Parameter | Symbol | min | typ | max | Unit | Remarks |
|-------|--|--------------|-----|------|-----|---------|--|
| 2.2.1 | Supply current | I_S | 3 | 6.8 | 9 | mA | - |
| 2.2.2 | Supply current @ 3.3V | I_{SVmin} | 3 | 6.7 | 8 | mA | $V_S=3.3V$ |
| 2.2.3 | Supply current @ 24V | I_{Smax} | 3 | 7 | 9.5 | mA | $V_S=24V$ $R_{Series} \geq 200\Omega$ |
| 2.2.4 | Output saturation voltage | V_{Qsat} | | 0.25 | 0.6 | V | $I_Q=20mA$ |
| 2.2.5 | Output leakage current | I_{Qleak} | | 0.1 | 10 | μA | $V_Q=18V$ |
| 2.2.6 | Current limit for short-Circuit protection | I_{Qshort} | 30 | 60 | 80 | mA | - |
| 2.2.7 | Junction temperature limit for output protection | T_{prot} | 195 | 210 | 230 | °C | - |
| 2.2.8 | Output rise time TLE4925C (PG-SSO-3-9) | t_r^3 | 4 | 12 | 20 | μs | $V_{Load} = 4.5$ to $24V$ $R_{Load} = 1.2k\Omega$; $C_{Load} = 4.7nF$ included in package. |
| | TLE4925 (PG-SSO-3-6) | | 4 | 12 | 20 | μs | |

³ value of capacitor: $4.7nF \pm 10\%$; (excluded drift due to temperature); ceramic: X7R; maximum voltage: 100V. The rise time is defined as the time between the 10 and 90% value.

| | | | | | | | |
|--------|--|---------------------|-------|-------|------------------------|--------------------------------|---|
| 2.2.9 | Output fall time TLE4925C (PG-SSO-3-9) | t_f^4 | 0.5 | 0.9 | 1.3 | μs | $V_{\text{Load}} = 5\text{V}$ $V_{\text{Load}} = 12\text{V}$ $R_{\text{Load}} = 1.2\text{k}\Omega$; $C_{\text{Load}} = 4.7\text{nF}$ included in package. |
| | 0.65 | | 1.15 | 1.65 | μs | | |
| | TLE4925 (PG-SSO-3-6) | | 0.5 | 0.9 | 1.3 | μs | $V_{\text{Load}} = 5\text{V}$ $V_{\text{Load}} = 12\text{V}$ $R_{\text{Load}} = 1.2\text{k}\Omega$; $C_{\text{Load}} = 4.7\text{nF}$ external capacitor. |
| | | | 0.65 | 1.15 | 1.65 | μs | |
| 2.2.10 | delay time Falling edge Rising edge | t_d | 7 | 12.5 | 18 20^5 25^6 | μs μs | Only valid for $T_j=25^\circ\text{C}$. $T_j=-40^\circ\text{C} - T_j=175^\circ\text{C}$ $T_j=-40^\circ\text{C} - T_j=175^\circ\text{C}$ Higher magnetic slopes and overshoots reduce t_d , because the signal is filtered internal. ⁷ |
| 2.2.11 | Temperature drift of delay time of output to magnetic edge | Δt_d | -6 | 3^8 | 6 | μs | Time over specified temperature range; not additional to t_d |
| 2.2.12 | Frequency range | f | 0.001 | | 8 | kHz | Operation below 1Hz^9 |
| 2.2.13 | Oscillator frequency | f_{OSC} | 1.08 | 1.34 | 1.68 | MHz | - |
| 2.2.14 | Offset recalibration time after last output change | t_{reset} | 625 | 780 | 970 | ms | Output locked to state before recalibration |
| 2.2.15 | Clamping voltage V_S -Pin | V_{Sclamp} | 24 | 27.5 | | V | $I_S = 20\text{mA} < 5\text{min}$. |
| 2.2.16 | Clamping voltage Q- Pin | V_{Qclamp} | 24 | 27.5 | | V | $I_Q = 20\text{mA} < 5\text{min}$. |
| 2.2.17 | Analog reset voltage | V_{sReset} | | 2.35 | 2.9 | V | - |

Note: The listed AC/DC and magnetic characteristics are ensured over the operating range of the integrated circuit. Typical characteristics specify mean values expected over the production spread. If not other specified, typical characteristics apply at $T_j = 25^\circ\text{C}$ and $V_S = 12\text{V}$.

⁴ see footnote 3.

⁵ only valid for the falling edge.

⁶ Not subject to production test-verified by design/characterisation

⁷ measured with a sinusoidal-field with 10mTpp and a frequency of 1kHz .

⁸ related to $T_j = 175^\circ\text{C}$.

⁹ output will switch if magnetic signal is changing more that $2x |\Delta B_{\text{min}}|$ within offset recalibration time even below 1Hz once per magnetic edge, increased phase error is possible

2.3 Magnetic Characteristics in Running Mode

| No. | Parameter | Symbol | min | typ | max | Unit | Remarks |
|-------|---|---------------------|------|-----|-----|------|-----------------------------------|
| 2.3.1 | Bias preinduction | B_0 | -500 | | 500 | mT | - |
| 2.3.2 | Differential bias induction | ΔB_0 | -30 | | 30 | mT | - |
| 2.3.3 | Minimum signal amplitude | $ \Delta B_{\min} $ | 0.55 | | 1.5 | mT | |
| 2.3.4 | Maximum signal amplitude | $ \Delta B_{\max} $ | | | 100 | mT | Additional to B_0 ¹⁰ |
| 2.3.5 | Resistivity against mechanical stress (piezo) | $ \Delta B_{\min} $ | -0.2 | | 0.2 | mT | F= 2N |

Note: The listed characteristics are ensured over the operating range of the integrated circuit. Typical characteristics specify mean values expected over the production spread. If not otherwise specified, typical characteristics apply at $T_j=25^\circ\text{C}$ and the given supply voltage.

3.1 Self-calibration Characteristics

| No. | Parameter | Symbol | min | typ | max | Unit | Remarks |
|-------|---|--------------------|-----|-------------------------------|-----|------|--|
| 3.1.1 | No. of magnetic edges for first output switching | n_{Start} | | | 2 | - | latest 2 nd magnetic edge will cause output switching |
| 3.1.2 | No. of magnetic edges to enter calibrated mode | n_{Calib} | | | 6 | - | Low phase accuracy permitted. See 3.1.7 7 th edge with high accuracy. Valid for sinusoidal signal without noise influence |
| 3.1.3 | Duty cycle in running mode ¹¹ | Dty | 45 | 50 | 55 | % | $\Delta B_{\text{pp}} = 10\text{mT}$ ideal sinusoidal input signal ($T_j=25^\circ\text{C}$) |
| | | | 40 | 50 | 60 | % | $\Delta B_{\text{pp}} = 10\text{mT}$ ideal sinusoidal input signal ($-40^\circ\text{C} \leq T_j < 175^\circ\text{C}$) |
| 3.1.4 | Signal jitter in running mode; 1 sigma value ⁵ | σ_1 | | $\leq \pm 0.11$ ¹² | | % | $\Delta B_{\text{pp}} = 10\text{mT}$ ideal sinusoidal input signal; $T_j < 150^\circ\text{C}$ |

¹⁰ exceeding this limit might result in decreased duty cycle performance. With higher values the internal measured signal will be clipped. This will decrease the phase accuracy.

¹¹ this corresponds to a $\Delta B_0 = 0\text{mT}$ (magnetic offset).

¹² depends largely on $|\Delta B_{\min}|$ magnetic signal steepness and also on frequency.

| | | | | | | | |
|-------|---|-------------------|--|-----------------|--|---------------|--|
| | | σ^2 | | $\leq \pm 0.16$ | | % | $\Delta B_{PP} = 10\text{mT}$ ideal sinusoidal input signal; $150^\circ\text{C} \leq T_j < 175^\circ\text{C}$ |
| 3.1.5 | Signal Jitter in running mode at power supply of $V_s=13\text{V}$ and ripple $\pm 3\text{V}$; 1 sigma value* | σ^3 | | $\leq \pm 0.11$ | | % | $\Delta B_{PP} = 10\text{mT}$ ideal sinusoidal input signal; $T_j < 150^\circ\text{C}$ |
| 3.1.6 | Effective noise value of the magnetic switching points, 1 sigma value | B_{neff} | | 25 | | μT | $T_j = 25^\circ\text{C}$; The magnetic noise is normal distributed, nearly independent to frequency and without sampling noise or digital noise effects. The typical value represents the rms-value here and corresponds therefore to 1σ probability of normal distribution. Consequently a 3σ value corresponds to 0.3% probability of appearance. |
| | | | | | | 70 | μT |
| 3.1.7 | Uncalibrated phase error Magnetic edge 1-2 After 3 rd edge Magnetic edge 1-3 | | | | | ° | Related to calibrated switching behaviour. $\Delta B_{PP} = 10\text{mT}$ ideal sinusoidal input signal ¹³ Magnetic fields close to $2x \Delta B_{\text{min}} $ |
| 3.1.8 | Frequency distribution of signal jitter | | Jitter shall be distributed like white noise | | | | - |

¹³ smaller phase errors are possible at higher signal amplitudes, because sinus signal changes to a more rectangle signal.

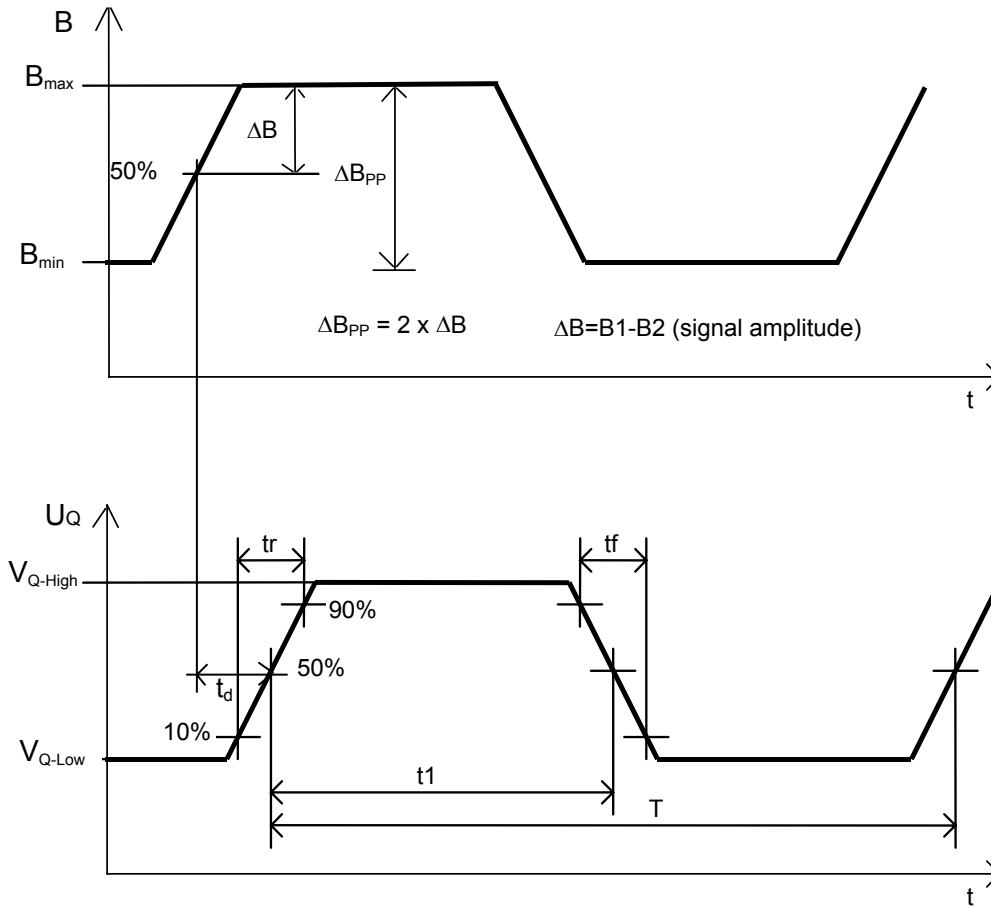
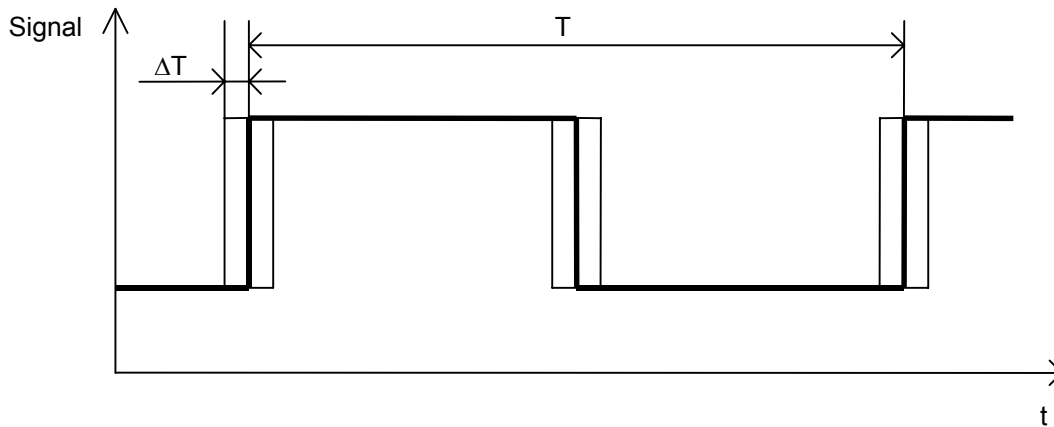


Figure 4 Switching direction



$$\sigma_1 \dots \sigma_3 = \frac{1}{T} \cdot \sqrt{\frac{1}{(n-1)} \cdot \sum (\Delta T)^2}$$

measurement condition: $n \geq 1000$

Figure 5 Definition of signal jitter

Application Configurations

Two possible applications are shown in **Figure 6** and **Figure 7** (Toothed and Magnet Wheel).

The difference between two-wire and three-wire application is shown in **Figure 10** for the TLE4925C and in **Figure 11** for the TLE4925.

Gear Tooth Sensing

In the case of ferromagnetic toothed wheel application the IC has to be biased by the south or north pole of a permanent magnet (e.g. SmCO₅ (Vacuumschmelze VX145)) with the dimensions 8 mm × 5 mm × 3 mm) which should cover both Hall probes.

The maximum air gap depends on

- the magnetic field strength (magnet used; pre-induction) and
- the toothed wheel that is used (dimensions, material, etc.; resulting differential field).

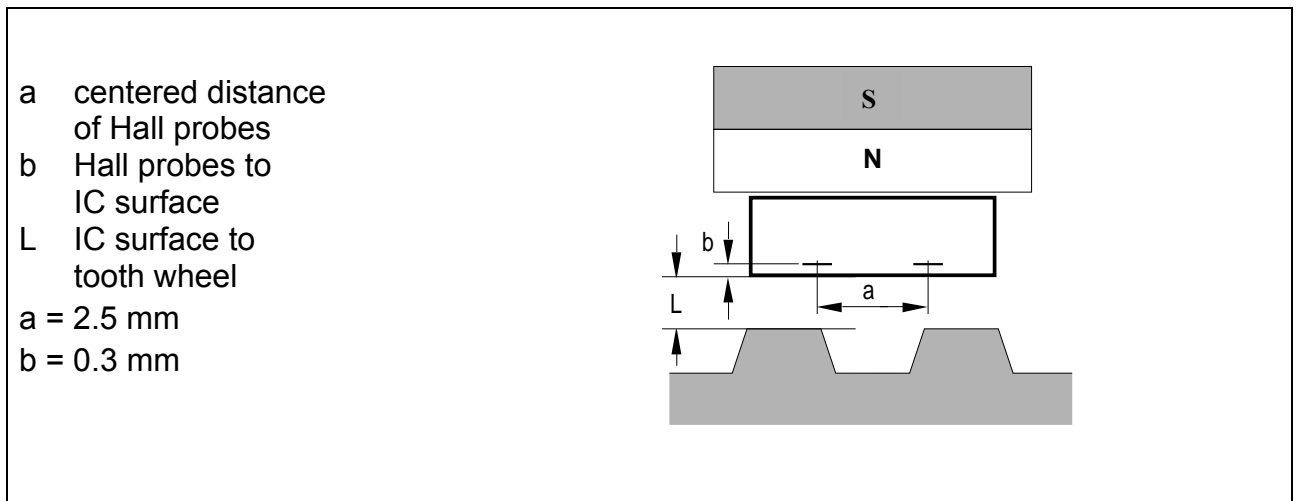


Figure 6 Sensor Spacing

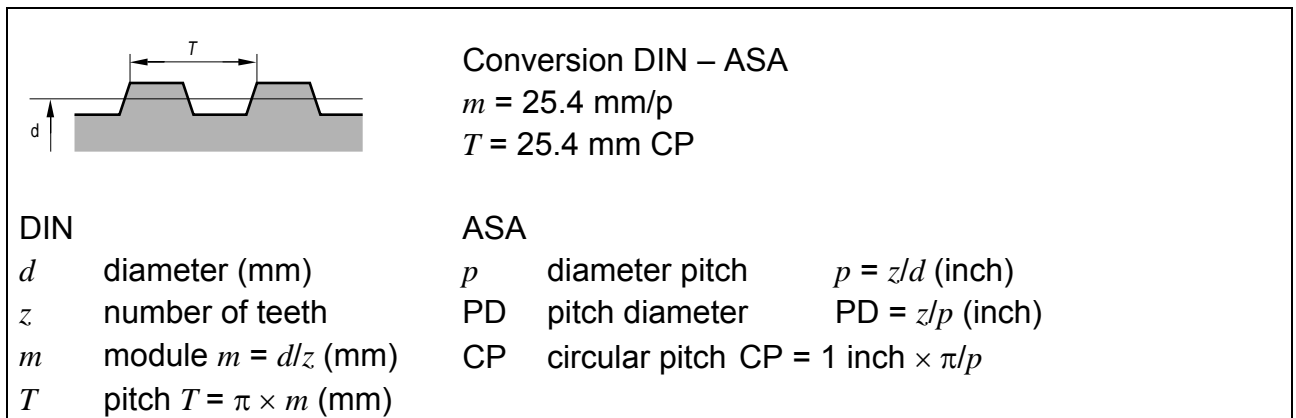


Figure 7 Toothed Wheel Dimensions

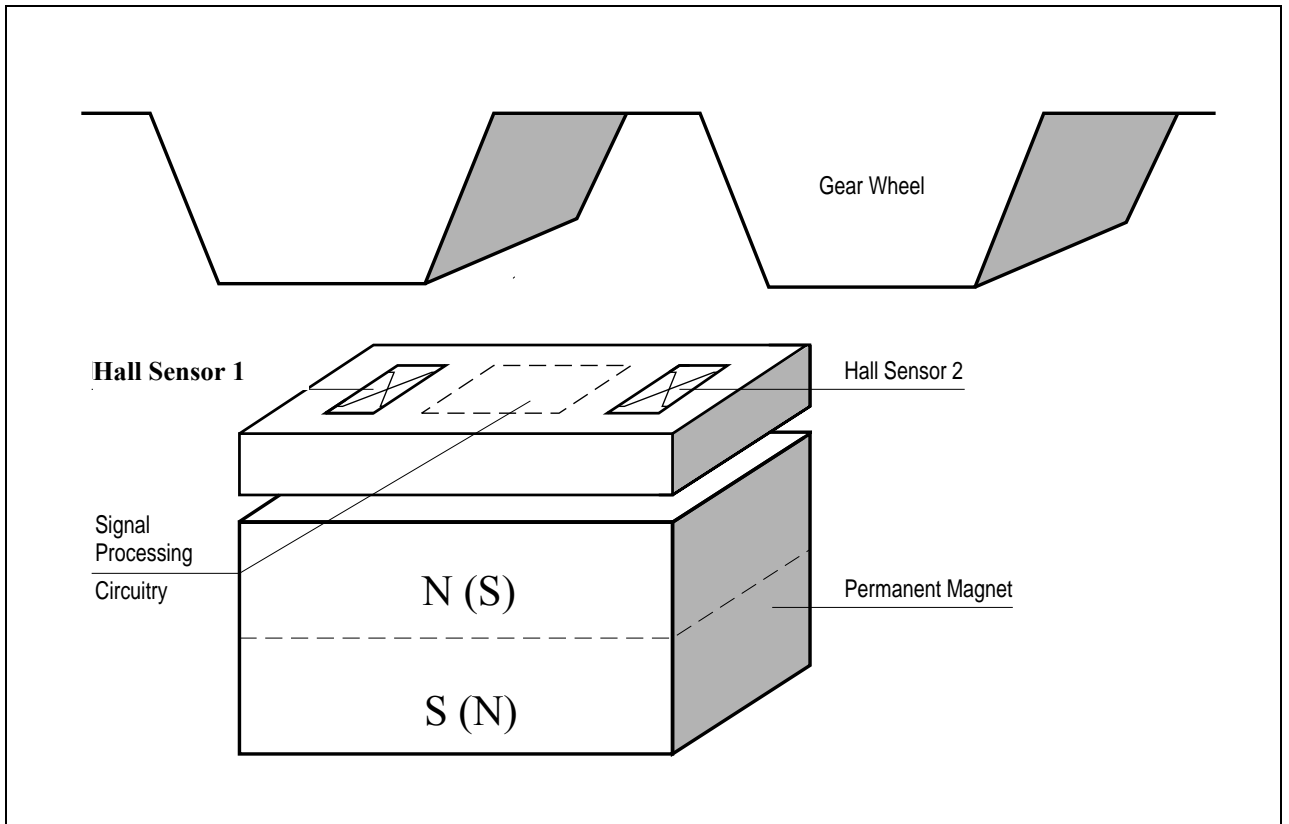


Figure 8 TLE4925/TLE4925C, with Ferromagnetic Toothed Wheel

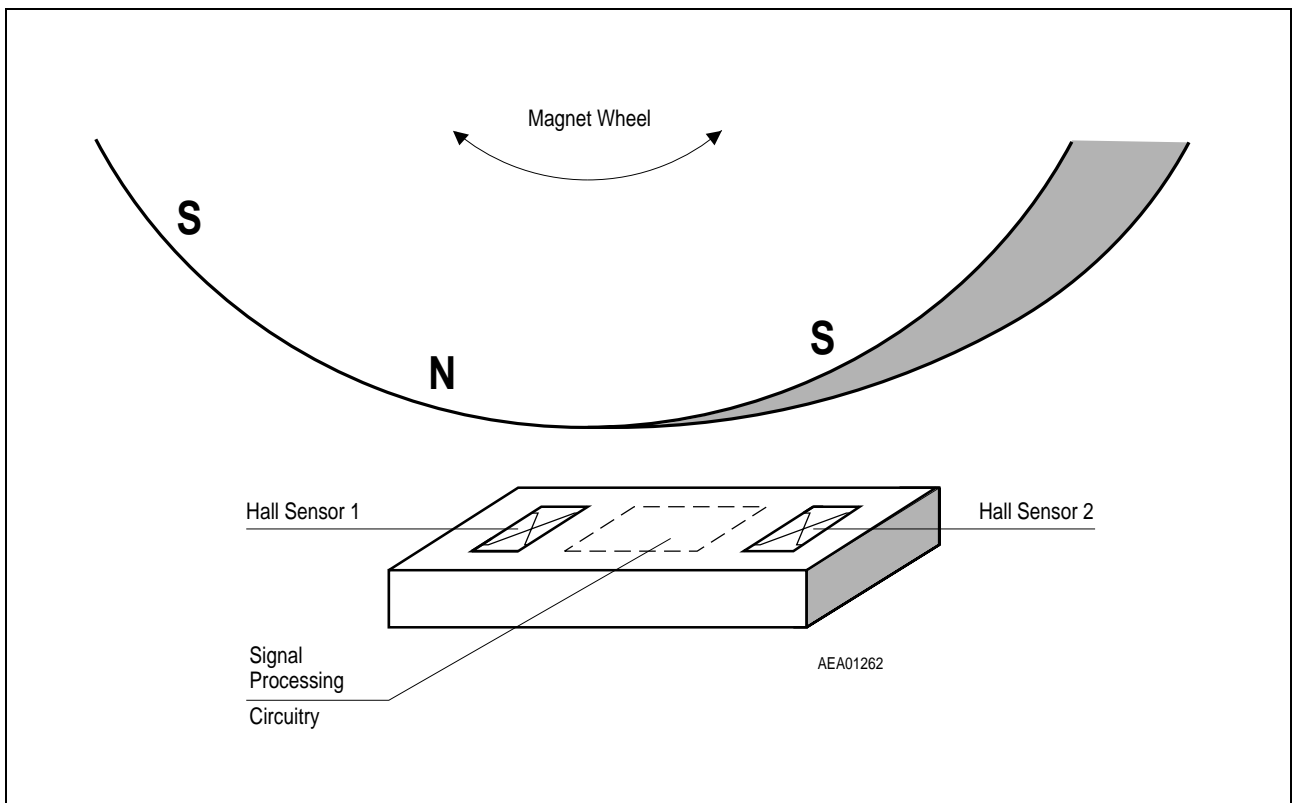


Figure 9 TLE4925/TLE4925C, with Magnet Wheel

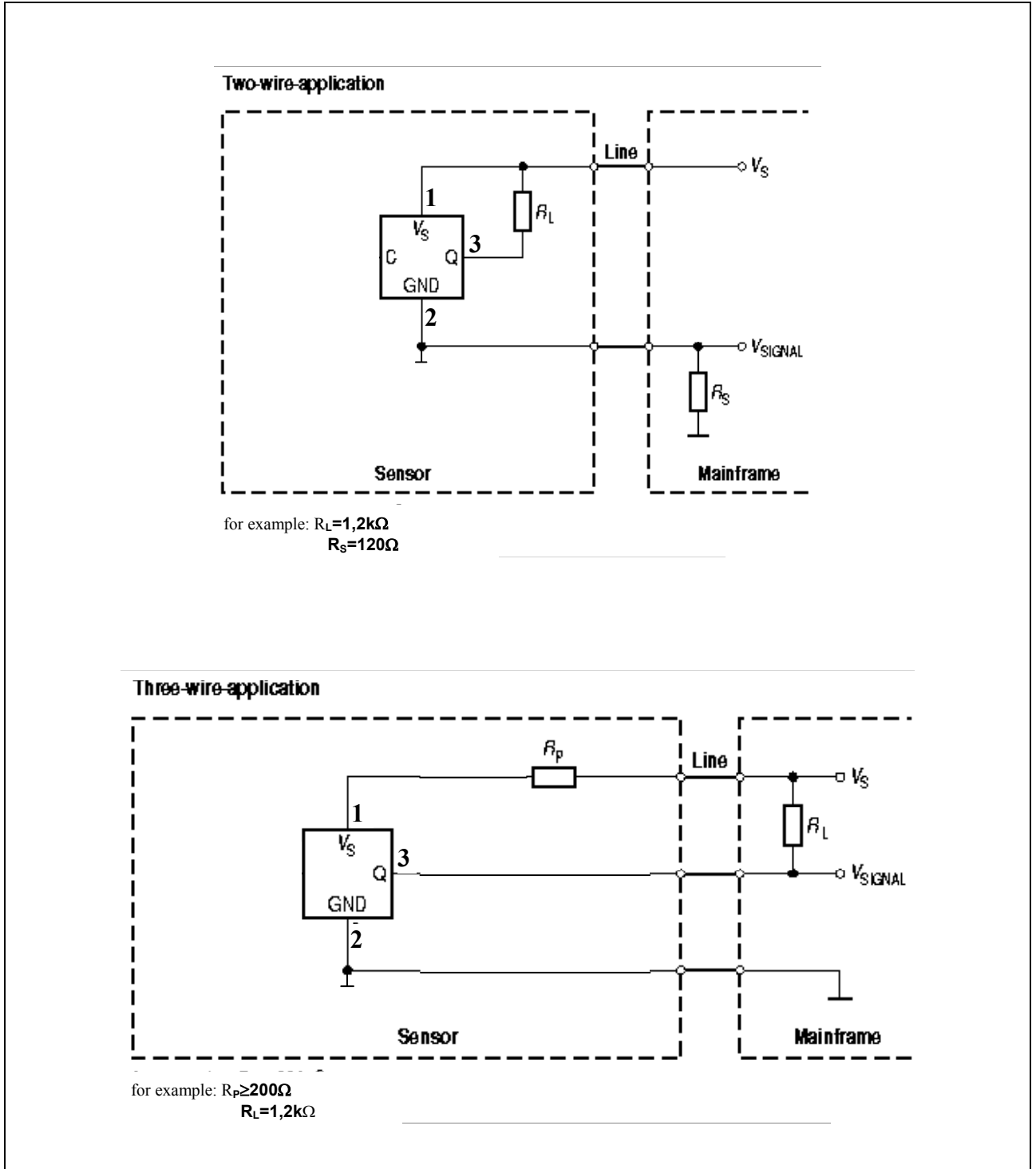


Figure 10 Application Circuits TLE4925C (capacitors added in package)

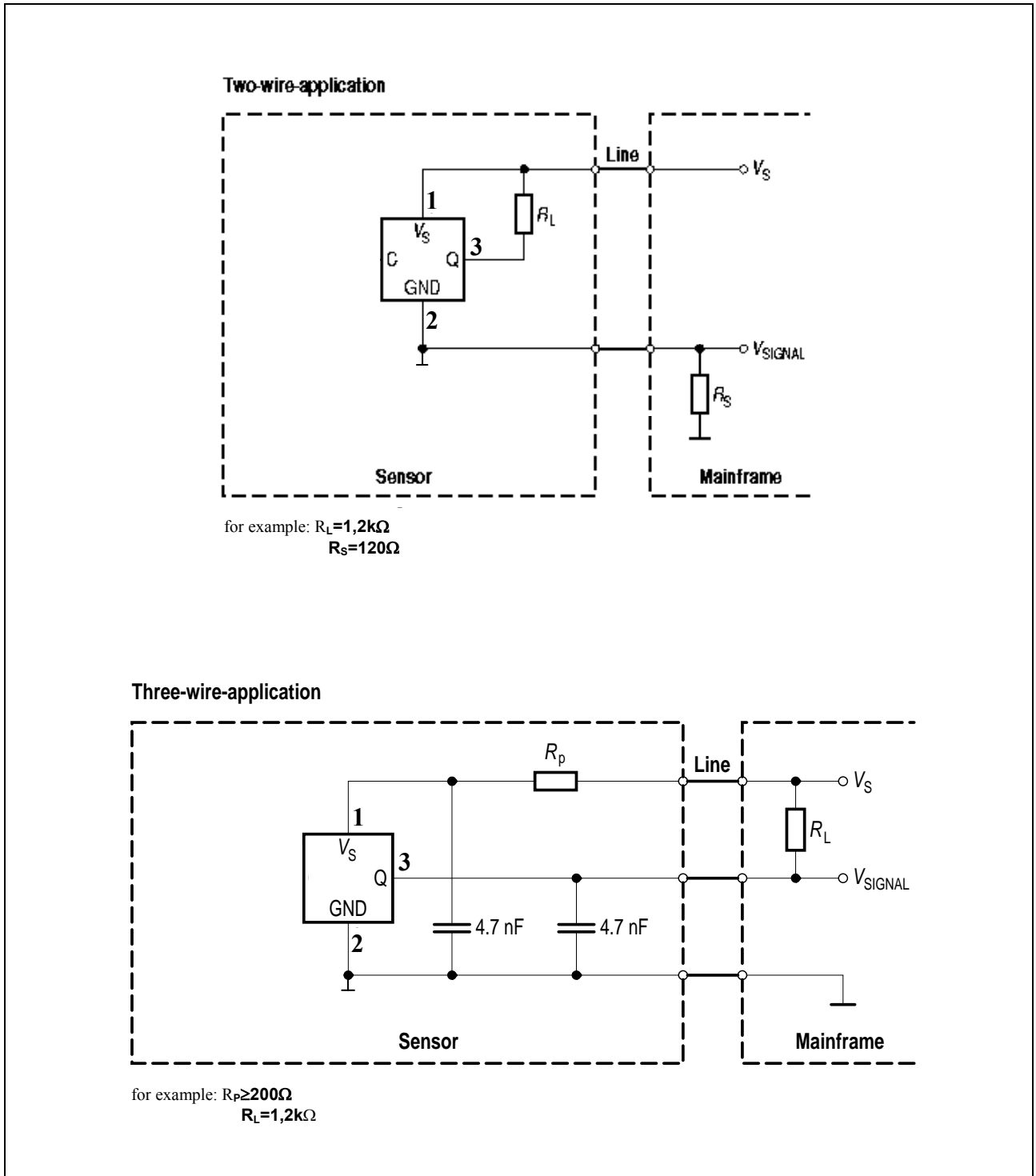


Figure 11 Application Circuits TLE4925 (capacitors to be added externally)

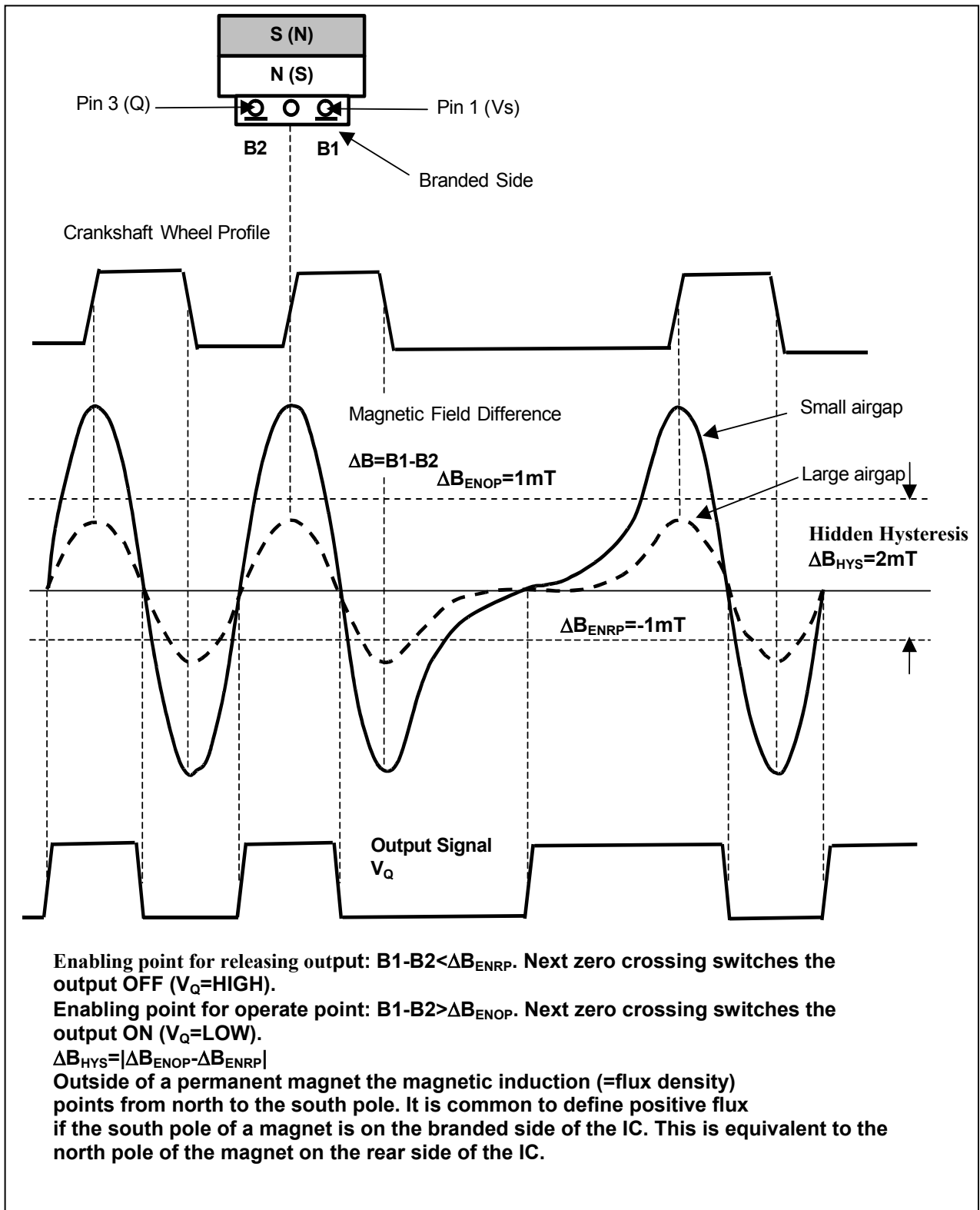
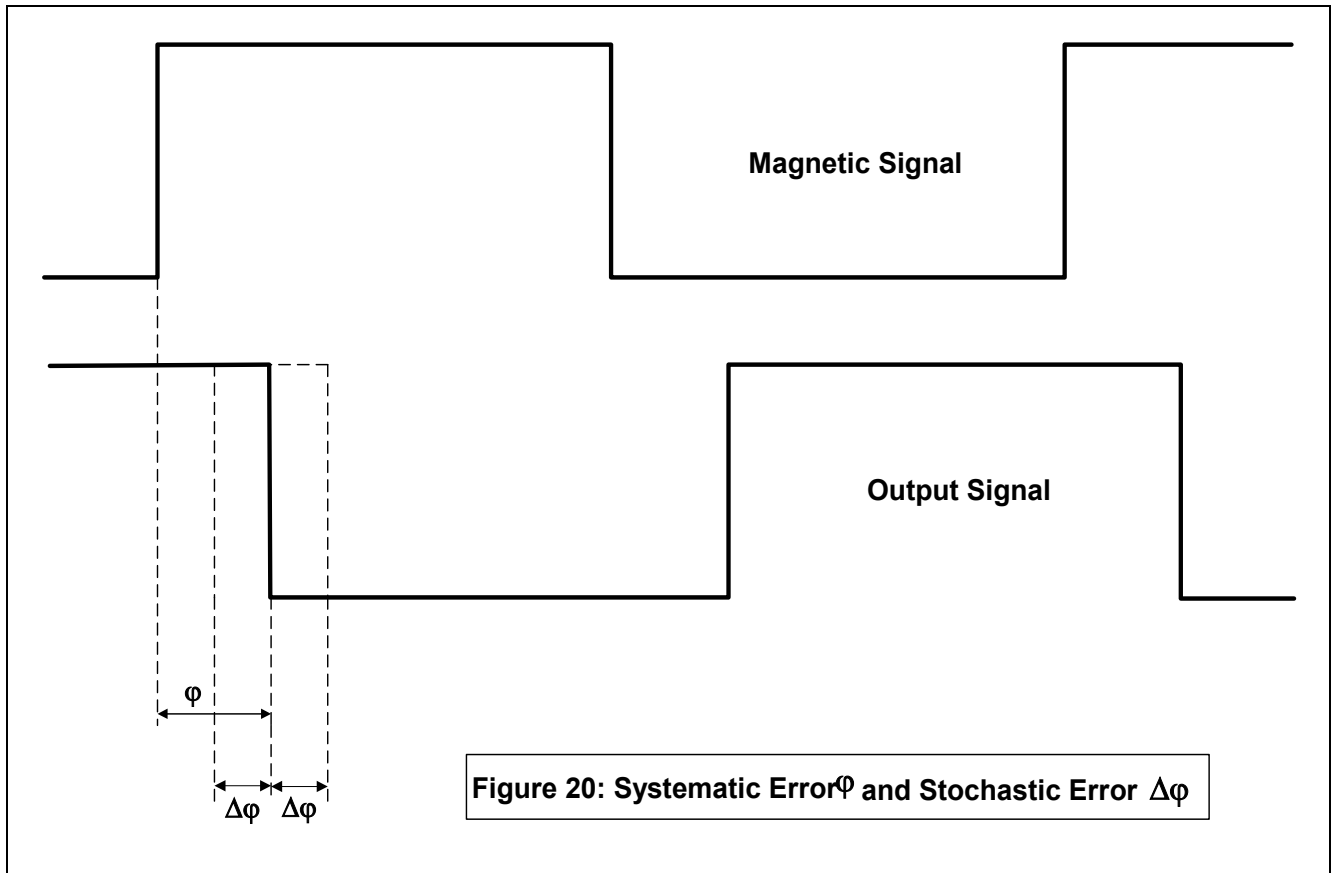


Figure 12 System Operation with hidden hysteresis

Appendix: Calculation of mechanical errors:



Systematic Phase Error φ

The systematic error comes in because of the delay-time between the threshold point and the time when the output is switching. It can be calculated as follows:

$$\varphi = \frac{360^\circ \cdot n}{60} \cdot t_d$$

- φ ... systematic phase error in $^\circ$
- n ... speed of the camshaft-wheel in min^{-1}
- t_d ... delay time (see specification) in sec

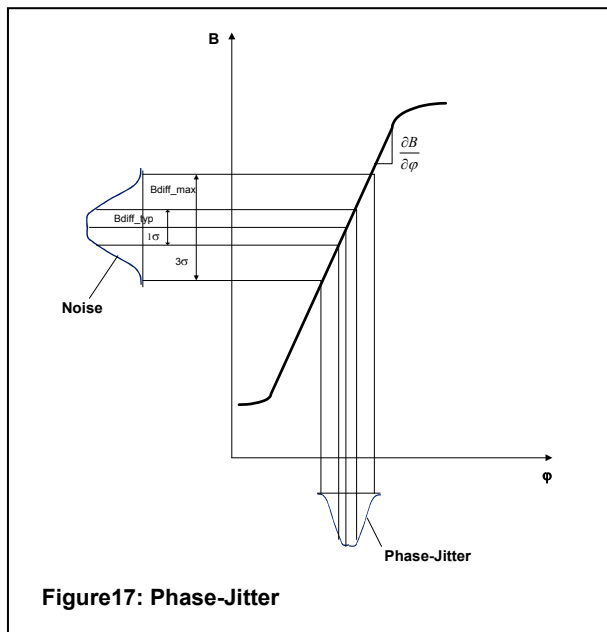
Systematic Phase Error $\Delta\varphi$

The systematic phase error includes the error due to the variation of the delay time with temperature and the error caused by the resolution of the threshold. It can be calculated in the following way:

$$\Delta\varphi_d = \frac{360^\circ \cdot n}{60} \cdot \Delta t_d$$

- $\Delta\varphi_d$... systematic phase error due to the variation of the delay time over temperature in $^\circ$
 n ... speed of the camshaft wheel in min^{-1}
 Δt_d ... variation of delay time over temperature in sec

Jitter (Repeatability)



The phase jitter is normally caused by the analogue system noise. If there is an update of the offset-DAC due to the algorithm, what could happen after each tooth, then an additional step in the phase occurs (see description of the algorithm). This is not included in the following calculations. The noise is transformed through the slope of the magnetic edge into a phase error. The phase jitter is determined by the two formulas:

$$\varphi_{Jitter_typ} = \frac{\partial\varphi}{\partial B} \cdot (B_{neff_typ})$$

$$\varphi_{Jitter_max} = \frac{\partial\varphi}{\partial B} \cdot (B_{neff_max})$$

| | | |
|--------------------------------------|-----|---|
| $\varphi_{\text{Jitter_typ}}$ | ... | typical phase jitter at $T_j=25^\circ\text{C}$ in $^\circ$ (1Sigma) |
| $\varphi_{\text{Jitter_max}}$ | ... | maximum phase jitter at $T_j=175^\circ\text{C}$ in $^\circ$ (3Sigma) |
| $\frac{\partial\varphi}{\partial B}$ | ... | inverse of the magnetic slope of the edge in $^\circ/T$ |
| $B_{\text{neff_typ}}$ | ... | typical value of B_{diff} in T (1 σ -value at $T_j=25^\circ\text{C}$) |
| $B_{\text{neff_max}}$ | ... | maximum value of B_{diff} in T (3 σ -value at $T_j=175^\circ\text{C}$) |

Example:

Assumption:

| |
|--|
| $n = 4500 \text{ min}^{-1}$ |
| $t_d = 14 \mu\text{s}$ |
| $\Delta t_d = \pm 3 \mu\text{s}$ |
| $\frac{\partial B}{\partial \varphi} = 3 \text{ mT/}^\circ$ |
| $B_{\text{neff_typ}} = \pm 40 \mu\text{T}$ (1 σ -value at $T_j=25^\circ\text{C}$) |
| $B_{\text{neff_max}} = \pm 210 \mu\text{T}$ (3 σ -value at $T_j=175^\circ\text{C}$) |

| | | | |
|--------------|--|-----|--|
| Calculation: | $\varphi = 0.378^\circ$ | ... | systematic phase error |
| variation | $\Delta\varphi_d = \pm 0.081^\circ$ | ... | systematic phase error due to delay time |
| | $\varphi_{\text{Jitter_typ}} = \pm 0.013^\circ$ | ... | typical phase jitter (1 σ -value at $T_j=25^\circ\text{C}$) |
| | $\varphi_{\text{Jitter_max}} = \pm 0.07^\circ$ | ... | maximum phase jitter (3 σ -value at $T_j=175^\circ\text{C}$) |

4.1 Electro Magnetic Compatibility - (values depend on R_{Series} !)

Ref. ISO 7637-1; see test circuit of figure 4 and 5;

$\Delta B_{PP} = 10\text{mT}$ (ideal sinusoidal signal); $V_S = 13.5\text{V} \pm 0.5\text{V}$, $f_B = 1000\text{Hz}$; $T = 25^\circ\text{C}$; $R_{Series} \geq 200\Omega$;

| No. | Parameter | Symbol | Level/typ | Status |
|-------|--------------|-----------|------------|--------|
| 4.1.1 | Testpulse 1 | V_{EMC} | IV / -100V | C |
| | Testpulse 2 | | IV / 100V | C |
| | Testpulse 3a | | IV / -150V | A |
| | Testpulse 3b | | IV / 100V | A |
| | Testpulse 4 | | IV / -7V | A |
| | Testpulse 5 | | IV / 86.5V | C |

Note: Test criteria for status A: No missing pulse no additional pulse on the IC output signal plus duty cycle and jitter are in the specification limits.

Test criteria for status B: No missing pulse no additional pulse on the IC output signal. (Output signal "OFF" means switching to the voltage of the pull-up resistor).

Test criteria for status C: One or more parameter can be out of specification during the exposure but returns automatically to normal operation after exposure is removed.

Test criteria for status E: IC destroyed.

Ref. ISO 7637-3; TP 1 and TP 2 ref. DIN 40839-3; see test circuit of figure 4 and 5;

$\Delta B_{PP} = 10\text{mT}$ (ideal sinusoidal signal); $V_S = 13.5\text{V} \pm 0.5\text{V}$, $f_B = 1000\text{Hz}$; $T = 25^\circ\text{C}$; $R_{Series} \geq 200\Omega$;

| No. | Parameter | Symbol | Level/typ | Status |
|-------|--------------|-----------|-----------|--------|
| 4.1.2 | Testpulse 1 | V_{EMC} | IV / -30V | A |
| | Testpulse 2 | | IV / 30V | A |
| | Testpulse 3a | | IV / -60V | A |
| | Testpulse 3b | | IV / 40V | A |

Ref. ISO 11452-3; see test circuit of figure 4 and 5; measured in TEM-cell;

$\Delta B_{PP} = 4\text{mT}$ (ideal sinusoidal signal); $V_S = 13.5\text{V} \pm 0.5\text{V}$, $f_B = 200\text{Hz}$; $T = 25^\circ\text{C}$; $R_{Series} \geq 200\Omega$;

| No. | Parameter | Symbol | Level/max | Remarks |
|-------|--------------------|----------------|-------------|-----------------|
| 4.1.3 | EMC field strength | $E_{TEM-Cell}$ | IV / 200V/m | AM=80%, f=1kHz; |

Note: Stresses above those listed here may cause permanent damage to the device. Exposure to absolute maximum rating conditions for extended periods may affect device reliability.

Test condition for the trigger window: $f_{B-field} = 200\text{Hz}$, $B_{pp} = 4\text{mT}$, vertical limits are $\pm 200\text{mV}$ and horizontal limits are $\pm 200\mu\text{s}$.

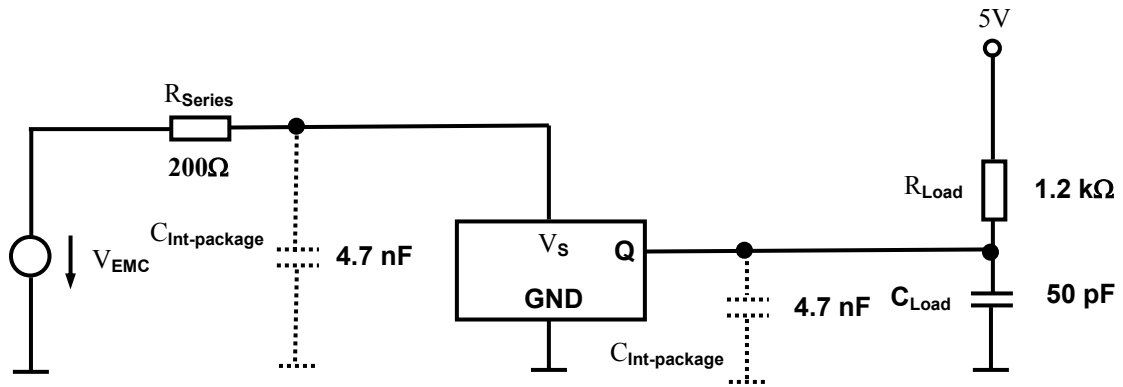


Figure 13: Test Circuit for EMC tests (TLE4925C) – PG-SSO-3-9 Package

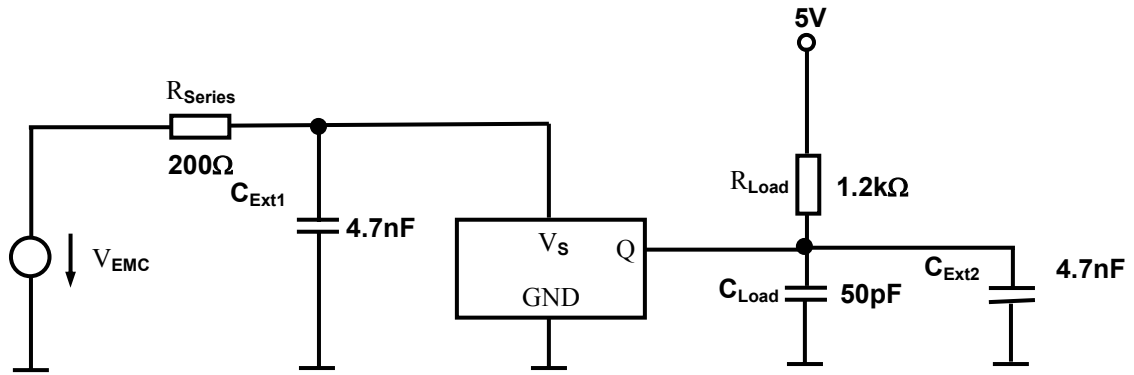


Figure 14: Test Circuit for EMC tests (TLE4925) – PG-SSO-3-6 Package

PG-SSO-3-9 (Plastic Green Single Small Outline)

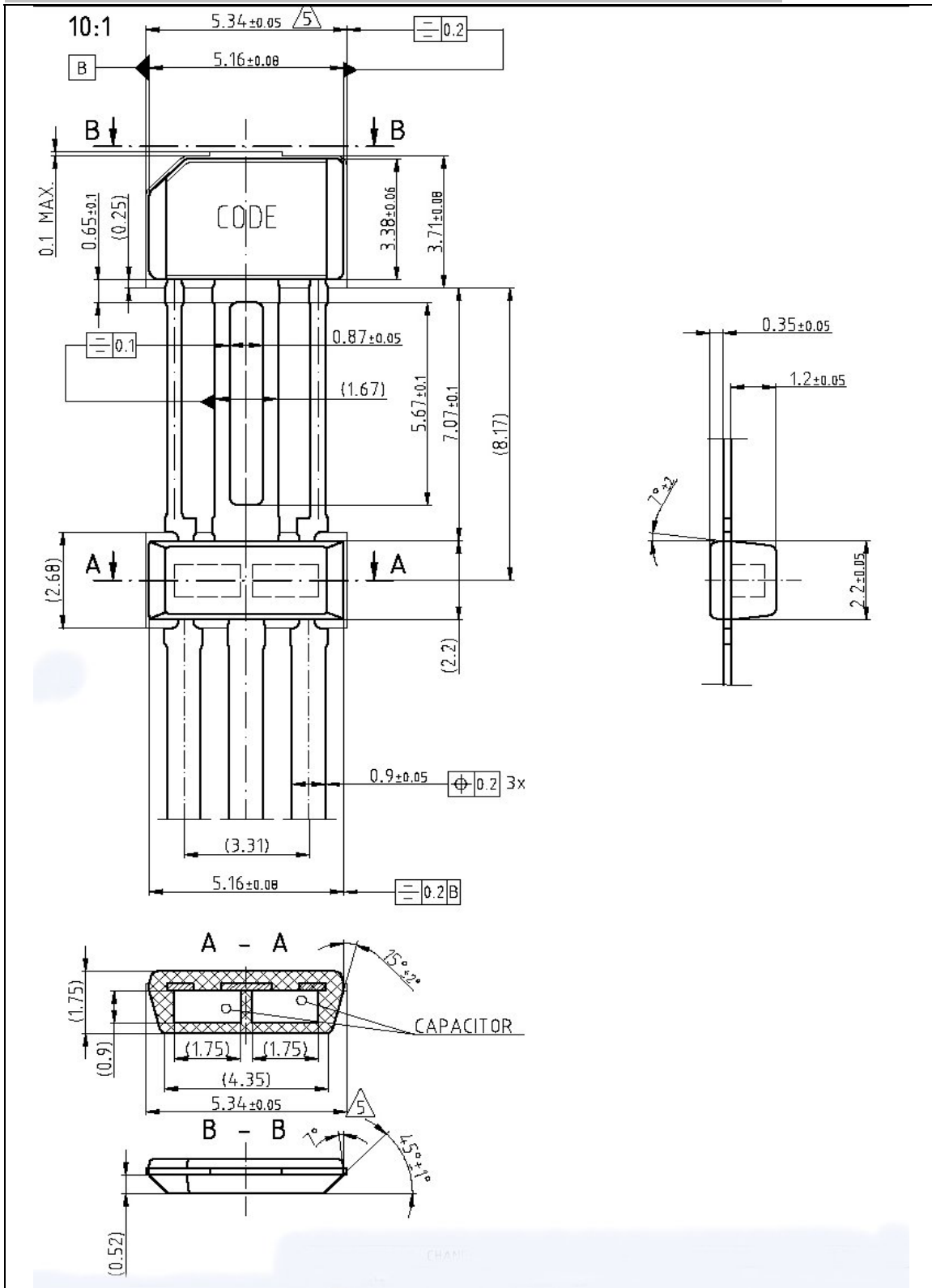


Figure 15 Package Dimensions (PG-SSO-3-9)

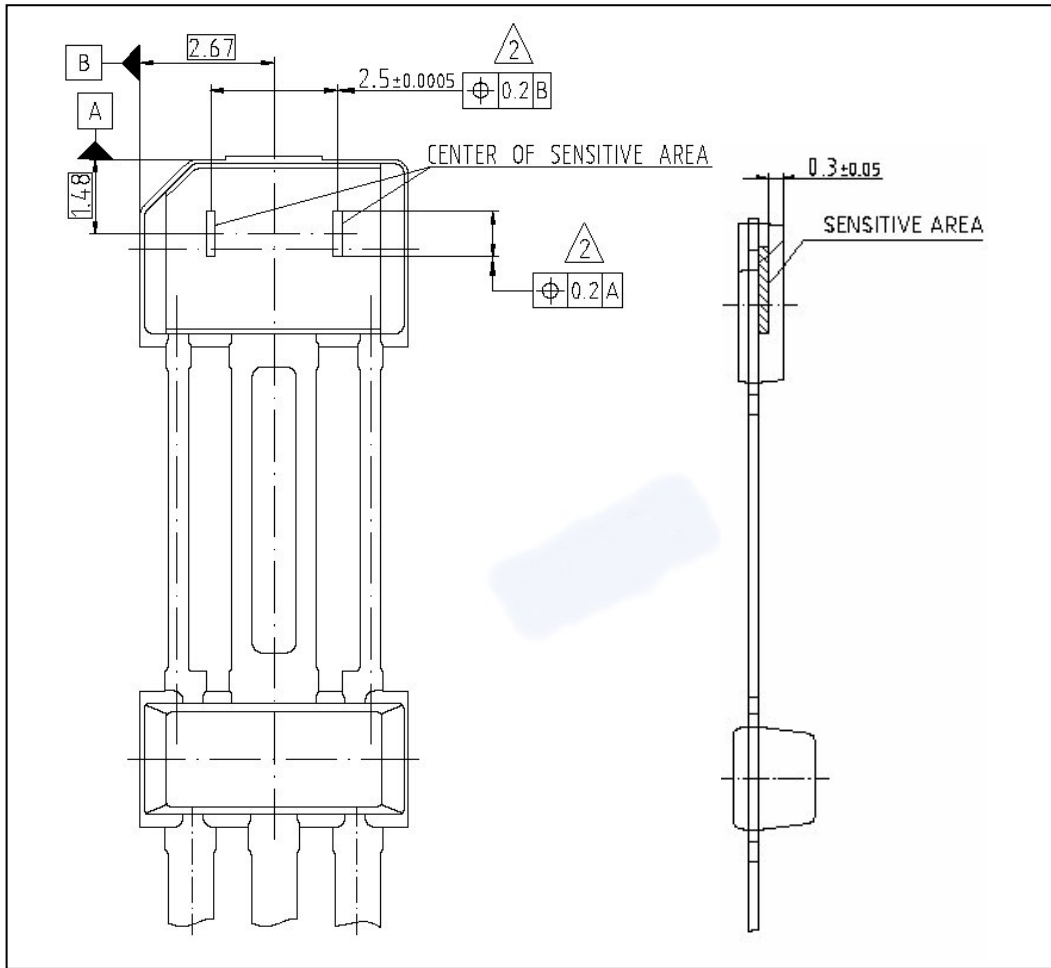


Figure 16 Hall probe spacing in the PG-SSO-3-9 package

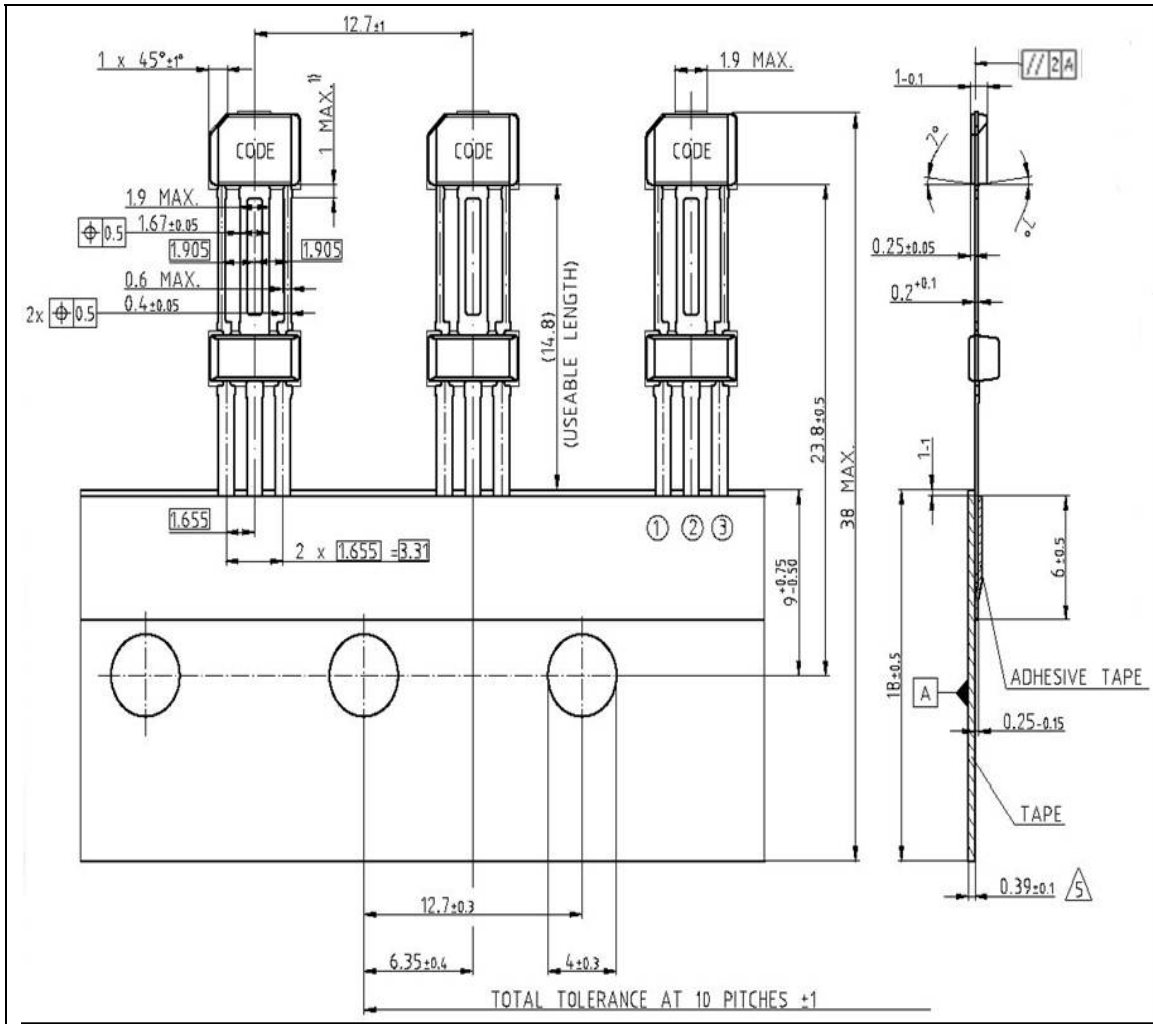


Figure 17 Tape Loading Orientation in the PG-SSO-3-9 package

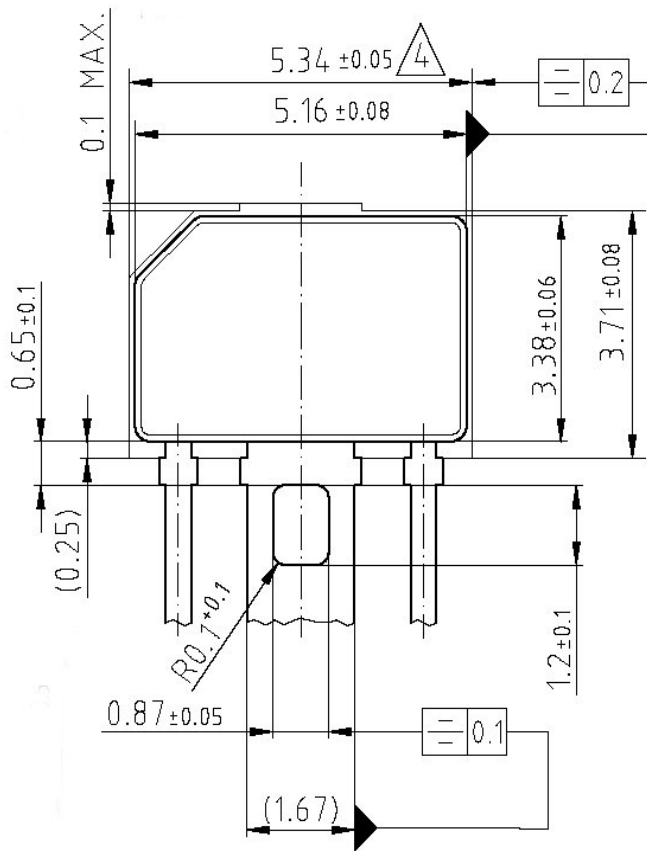
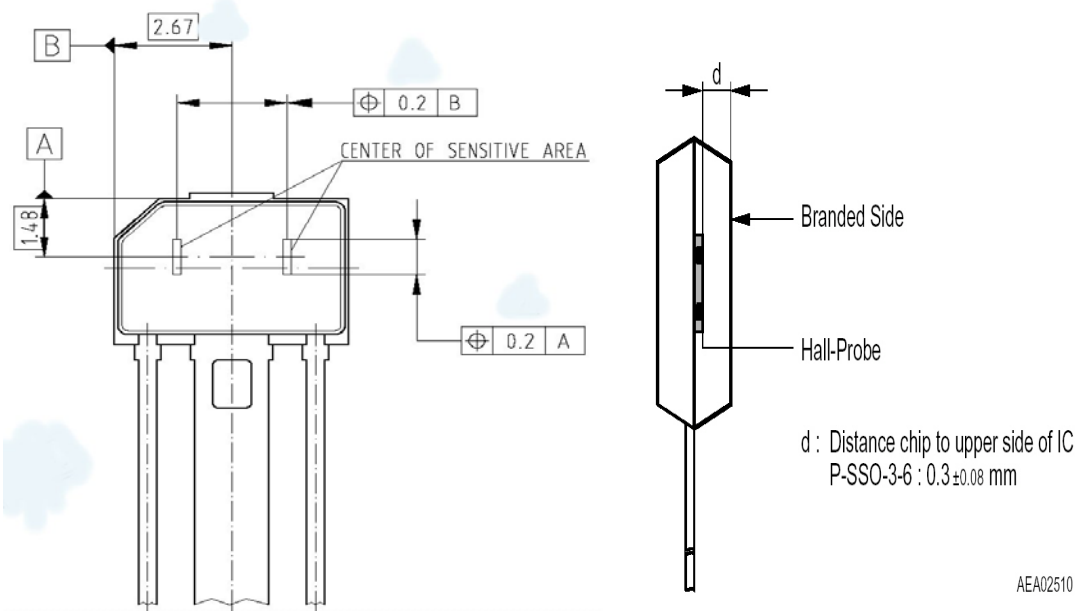


Figure 18 Package Dimensions (PG-SSO-3-6)



AEA02510

Figure 19 Hall probe spacing in the PG-SSO-3-6 package

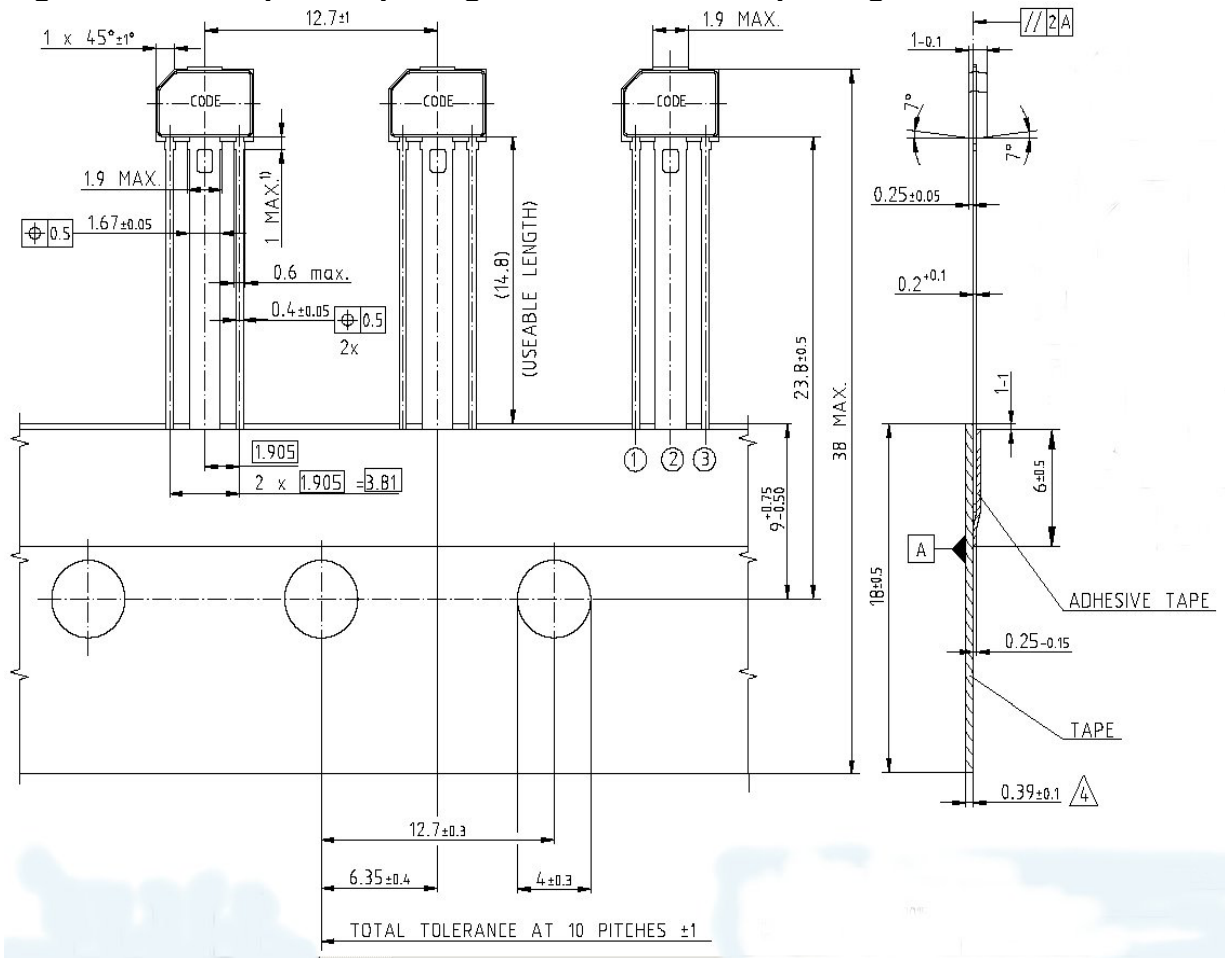


Figure 20 Tape Loading Orientation in the PG-SSO-3-6 package

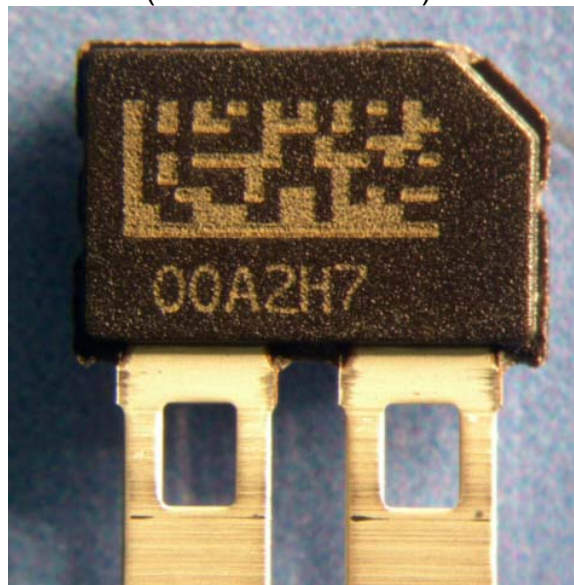
Appendix A: Marking & data matrix code information:

Product is RoHS (restriction of hazardous substances) compliant when marked with letter "G" in front or after the date code marking.

As mentioned in information note N° **136/03** a data matrix code with 8x18 fields according to the ECC200 standard may be used for sensor production. Furthermore the marking technique on the front side of the device may be changed from a mask to a laser writing equipment. The information content (date code and device type) will hereby not be changed.

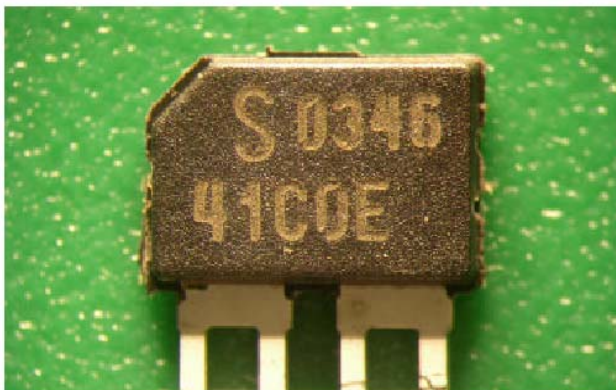
Please refer to your key account team or regional sales responsible if you need further information.

Example for data matrix code (rear side of sensor):



Comparison between mask writing vs. new laser writing:

Mask Lasering



Writing Lasering



Previous Version: 5.0

| Page | Subjects (major changes since last revision) |
|------|---|
| 6 | ESD-protection max. value changed from 8 to 6kV |
| 24 | Update package drawing: parallelism |
| 27 | Update comparison mask writing/laser writing |
| | |
| | |

Infineon Technologies AG**© Infineon Technologies AI SC****All Rights Reserved.**<http://www.infineon.com/products/sensors>**We Listen to Your Comments**

Any information within this document that you feel is wrong, unclear or missing at all?
Your feedback will help us to continuously improve the quality of this document.
Please send your proposal (including a reference to this document) to:

Feedback.sensors@infineon.com